

Mie resonance-based dielectric metamaterials

Increasing attention on metamaterials has been paid due to their exciting physical behaviors and potential applications. While most of such artificial material structures developed so far are based on metallic resonant structures, Mie resonances of dielectric particles open a simpler and more versatile route for construction of isotropic metamaterials with higher operating frequencies. Here, we review the recent progresses of Mie resonance-based metamaterials by providing a description of the underlying mechanisms to realize negative permeability, negative permittivity and double negative media. We address some potential novel applications.

Qian Zhao^{1,2}, Ji Zhou^{1,*}, Fuli Zhang³, Didier Lippens³

¹ State Key Lab of New Ceramics and Fine Processing, Department of Materials Science and Engineering, Tsinghua University, Beijing, PRC

² State Key Lab of Tribology, Department of Precision Instruments and Mechanology, Tsinghua University, Beijing, PRC

³ Institut d'Electronique de Micro-électronique et de Nanotechnologie, UMR CNRS 8520, University of Lille 1, Villeneuve d'Ascq Cedex, France

*E-mail: zhouji@mail.tsinghua.edu.cn

Metamaterials are artificial electromagnetic media structured on a scale much shorter than their operating wavelength. Under this condition they can be considered as homogeneous media whose electromagnetic properties rely mainly on the basic cell rather than periodic effects as it is the case for photonic crystal or more generally electromagnetic band gap material. Their basic cells are generally constituted of resonant inclusions which yield a π phaseshift in the material response above the resonant frequency. As a consequence, their effective permittivity and permeability can be negative either in separate or overlapping frequency bands, a unique and distinct property that is not observed in naturally occurring materials¹. For the latter condition they can be considered as double negative or negative index media hence

opening the effective parameter space, so that new functionalities in the light scattering can be envisaged.

Also recently, the achievement of near-zero or less than unity values of the effective permittivity and permeability was also recognized as one of the major goals of this research area. Great progress in electromagnetic metamaterials has been achieved for these unique physical properties and novel potential applications, such as negative refraction^{2,3}, perfect lens^{4,5} and cloaking⁶⁻⁸ have been shown. They have been experimentally demonstrated in a frequency range from the radio frequencies⁹ to millimeter waves¹⁰, infrared wavelengths¹¹⁻¹³, and visible optics¹⁴. Up to date, most of metamaterials are constructed with the use of sub-wavelength resonant metallic elements. For instance, the first left-handed

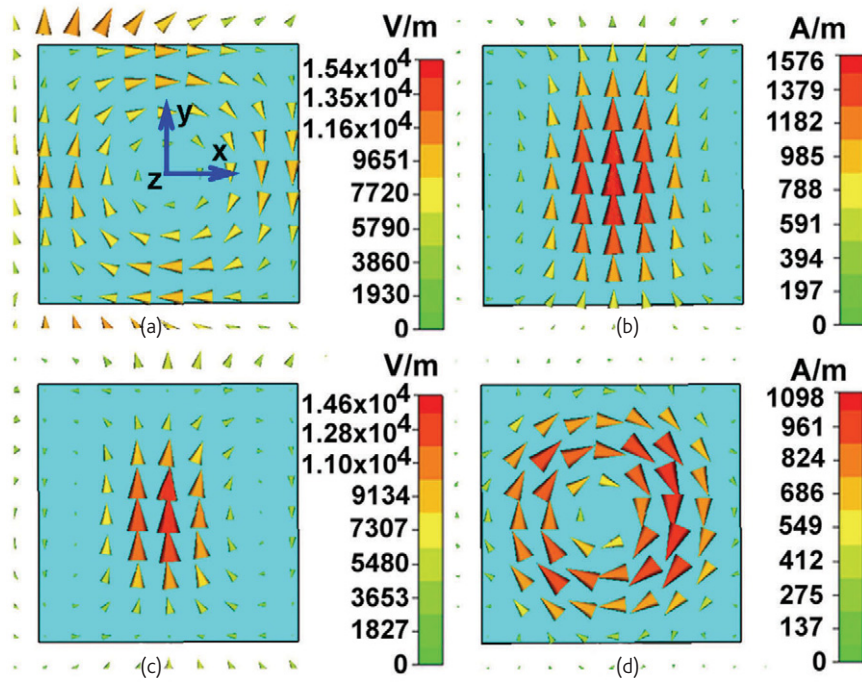


Fig. 1 Electric and magnetic field distribution in a dielectric cube with the magnetic field polarized along the z axis and electric field polarized along the y axis. (a) Electric field in the plane $z=0$ near the first Mie resonance. (b) Magnetic field in the plane $y=0$ near the first Mie resonance. (c) Electric field in the plane $z=0$ near the second Mie resonance. (d) Magnetic field in the plane $y=0$ near the second Mie resonance. (Reprinted with permission from³⁷. © 2008 American Physical Society.)

metamaterials (LHMs) with simultaneously negative permittivity and permeability have been fabricated by means of metallic split ring resonators (SRRs) and wires^{15, 16}, for tailoring the magnetic and electric responses, respectively. Other metallic elements, such as Ω -shaped structures^{17, 18}, U -shaped structures¹⁹, staplelike structures²⁰, paired rods²¹, dendritic²² and fishnet structures²³, are also successfully used to fabricate LHMs.

Usually, the metallic constitutive elements have conductive loss and anisotropic electromagnetic responses. Several authors have suggested methods^{24–26} to construct isotropic metamaterials by combining metallic SRRs and wires. However it is difficult to fabricate the bulk arrays of complex geometry with submicron or nanoscale sizes in order to generate a negative permeability effect at infrared and optical frequencies²⁷.

Recently, another route based on the interaction between electromagnetic waves and dielectric particles^{28, 29} was proposed to achieve the electric or magnetic resonances. The Mie resonances of dielectric inclusions provide a novel mechanism for the creation of magnetic or electric resonance based on displacement currents, and offer a simpler and more versatile route for the fabrication of isotropic metamaterials operating at higher frequencies. The progress on metallic elements-based metamaterials has been reviewed in many articles^{30–32} and books^{33, 34}. In this review, we focus on the scattering mechanisms based on Mie resonance in dielectric particles and describe the recent progress in these metamaterials including ferroelectric and polaritonic particles and their tunable behaviors.

Mie resonance of particles

From the viewpoint of scattering theory, all scattering objects can be represented by effective electric and/or magnetic polarizability densities. Light scattering by small (relative to the incident light wavelength) spherical particles is a fundamental topic in classical electrodynamics³⁵, and is based upon the exact Mie solution of the diffraction problem³⁶. The scattered field of a single isolated dielectric sphere with radius r_0 and relative refractive index n can be decomposed into a multipole series with the 2^m -pole term of the scattered electric field proportional to

$$a_m = \frac{n\Psi_m(nx)\Psi_m'(x) - \Psi_m(x)\Psi_m'(nx)}{n\Psi_m'(nx)\xi_m'(x) - \xi_m(x)\Psi_m'(nx)} \quad (1)$$

whereas the 2^m -pole term of the scattered magnetic field is proportional to

$$b_m = \frac{\Psi_m(nx)\Psi_m'(x) - n\Psi_m(x)\Psi_m'(nx)}{\Psi_m'(nx)\xi_m'(x) - n\xi_m(x)\Psi_m'(nx)} \quad (2)$$

where $x=k_0r_0$, k_0 is the free-space wavenumber, and $\Psi_m(x)$ and $\xi_m(x)$ are the Riccati-Bessel functions. The primes indicate derivation with respect to the arguments. The scattering coefficient a_m and b_m are related to the electric and magnetic responses of the sphere, respectively. From the Mie theory we can calculate the electric and magnetic dipole coefficients, a_1 and b_1 , respectively. From effective medium theory, we know that these are the multipole terms which contribute most significantly to the effective permittivity and

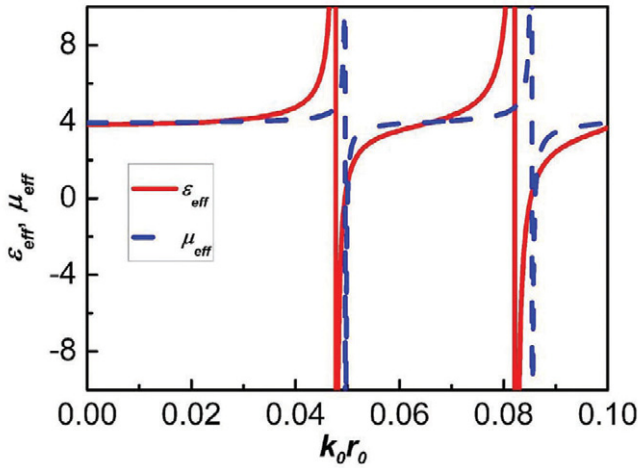


Fig. 2 Calculated effective permittivity ϵ_{eff} and permeability μ_{eff} of the magnetodielectric sphere arrays composite. (Reprinted with permission from²⁹. © 2003 IEEE.)

permeability of the particle composite. Since the magnetic response of a nonmagnetic particle is usually weak, it is important to strengthen the electromagnetic resonant behavior. For the lowest resonant frequencies of a_1 and b_1 , the sphere exhibits electric and magnetic dipoles. This conclusion can be assessed from the electromagnetic intensity distributions in a high dielectric ceramic cube for a plane incident wave propagating along the x axis³⁷ (Fig. 1). It can be seen that the electric or magnetic fields are mainly localized in the cubes. The azimuthal component of the displacement current inside each cube is greatly enhanced at the first Mie resonance (Fig. 1a) resulting in a large magnetic field along the z axis (Fig. 1b) which corresponds to the TE_{011} Mie resonance mode. At the second Mie resonance, the y component of the displacement current inside the cubes increases dramatically (Fig. 1c) and hence with a large magnetic field along the azimuth (Fig. 1d), which corresponds to the TM_{011} Mie resonance mode.

These electric and magnetic dipole resonances act as artificial ‘atoms’ which form the basis of new optical materials. In a material made up of a collection of such resonant particles, their combined scattering response can act like a material with almost arbitrary values of effective permittivity and permeability. This idea can be verified by using the model proposed in 1947 by Lewin³⁸ who considered the electromagnetic scattering properties of a composite material which was constituted of an array of lossless magnetodielectric spheres (ϵ_2 and μ_2) embedded in another background matrix (ϵ_1 and μ_1). The effective permittivity ϵ_{eff} and permeability μ_{eff} expressions based on Mie theory are as follows³⁸.

$$\epsilon_{eff} = \epsilon_1 \left(1 + \frac{3v_f}{\frac{F(\theta) + 2b_e - v_f}{F(\theta) - b_e}} \right) \quad (3)$$

$$\mu_{eff} = \mu_1 \left(1 + \frac{3v_f}{\frac{F(\theta) + 2b_m - v_f}{F(\theta) - b_m}} \right) \quad (4)$$

where

$$F(\theta) = \frac{2(\sin\theta - \theta \cos\theta)}{(\theta^2 - 1)\sin\theta + \theta \cos\theta} \quad (5)$$

$$b_e = \epsilon_1/\epsilon_2, \quad b_m = \mu_1/\mu_2 \quad (6)$$

The volume fraction of the spherical particles,

$$v_f = \frac{4}{3}\pi\left(\frac{r_0}{p}\right)^3, \quad \theta = k_0 r_0 \sqrt{\epsilon_2 \mu_2}, \quad r_0 \text{ and } p \text{ are the particle radius and}$$

the lattice constant, respectively. Eq 5 shows that $F(\theta)$ is a resonant function and becomes negative above resonance in some range of θ , resulting in the negative permittivity or permeability for negative values of $F(\theta)$ with a magnitude on the order of unity as given by Eqs. (3) and (4).

In Lewin’s model, the constitutive parameters were formulated only considering the spheres resonating either in the first or second resonant modes of the Mie series. This is because the higher order Mie resonances often occur at frequencies beyond the long wavelength limit, and thus the Clausius-Mossotti equation does not apply. Then, Jylha *et al.*³⁹ improved those formulations by taking into account the electric polarizabilities of spheres operating in the magnetic resonant modes.

Independent of Lewin’s model, O’Brien and Pendry²⁸ showed that a negative effective permeability can be obtained in a two-dimensional array of ferroelectric rods with the magnetic field polarized along the axes of the rods. Although the underlying physics is the same, the authors used another method⁴⁰ (transfer matrix method) to find the effective media values with similar conclusion. The aforementioned theoretical results show that a high permittivity microstructured medium can exhibit isotropic negative values of the effective permeability and permittivity.

Mie resonance as a new route for metamaterials

With the rapid development of LHMs, Lewin’s model was reconsidered and introduced into the realm of metamaterials to realize single and double negative media. Based on Lewin’s model, Holloway *et al.*²⁹ numerically demonstrated the feasibility of achieving simultaneously negative ϵ_{eff} and μ_{eff} in the magnetodielectric sphere arrays for wavelengths where the electric and magnetic resonances are excited in the spheres. Eqs. (3) and (4) show that ϵ_{eff} and μ_{eff} depend on the permeability and permittivity of the dielectric inclusions and host medium, as well as the volume fraction of spheres of radius r_0 . Fig. 2 shows ϵ_{eff} and μ_{eff} calculated for $v_f = 0.5$, $\epsilon_1 = \mu_1 = 1$, $\epsilon_2 = 40$, and

$\mu_2 = 200$ as a function of $k_0 r_0$. There are two regions where both ϵ_{eff} and μ_{eff} become negative with the bandwidths becoming narrower by decreasing the volume fraction v_f .

From a practical point of view, many kinds of materials and shapes of particles have been proposed in the literature to fabricate negative or less than unity permeability and permittivity dielectric metamaterials operating in different frequency regions. The designing ideas are summarized in the following.

Magnetic response

The realization of abnormal permeability is a tricky issue for various metamaterials, because the magnetic response of materials is usually weak, especially at infrared or visible frequencies. Lewin's model shows that two methods based on Mie resonance can be used to achieve a negative effective permeability effect. The first one is to use magnetodielectric inclusions with large values of permeability and permittivity. The second method is to use nonmagnetic dielectric particles with extremely large permittivity values. In the former case, two terms b_e and b_m in Eqs. (3) and (4) contribute to the negative permeability, while only b_e plays an important role for the latter. The possibility to use magnetodielectric particles has been numerically demonstrated²⁹. However a magnetodielectric particle with simultaneously large values of permittivity and permeability seems physically unattainable even in the microwave. Eq. (4) indicates that nonmagnetic spheres with very high permittivity values can also be employed to induce negative permeability and permittivity effects at the different Mie resonance frequencies.

Polaritonic materials, such as ionic solids and polar semiconductors, or ferroelectric materials can provide the large permittivity. For ferroelectric materials, their extreme high permittivity values can be preserved at least up to millimeter wavelengths⁴¹. At infrared frequencies however a roll-off of the dielectric constant is observed so that they cannot be used in this frequency range. In contrast, the lattice resonance in polaritonic crystals can be exploited to tailor the permittivity resonance at infrared and optical frequencies. As a consequence, the polaritonic resonance of crystals could be potentially used in the infrared spectral region. The relative permittivity is⁴²

$$\epsilon_r(\omega) = \epsilon(\infty) \left(1 + \frac{\omega_L^2 - \omega_T^2}{\omega_T^2 - \omega^2 - i\omega\gamma} \right), \quad (7)$$

where $\epsilon(\infty)$ is the high-frequency limit of the permittivity, ω_T and ω_L are the transverse and longitudinal optical phonon frequencies, and γ is the damping coefficient. Therefore, large values of $\epsilon_r(\omega)$ can be achieved near the transverse phonon frequency.

A three-dimensional dielectric composite consisting of an array of dielectric cubes [$\text{Ba}_{0.5}\text{Sr}_{0.5}\text{TiO}_3$ (BST)] with a relative permittivity of 1600 in a Teflon substrate was fabricated (Fig. 3a) to demonstrate the feasibility of this full dielectric metamaterial route. On this basis, isotropic negative values of the effective permeability were

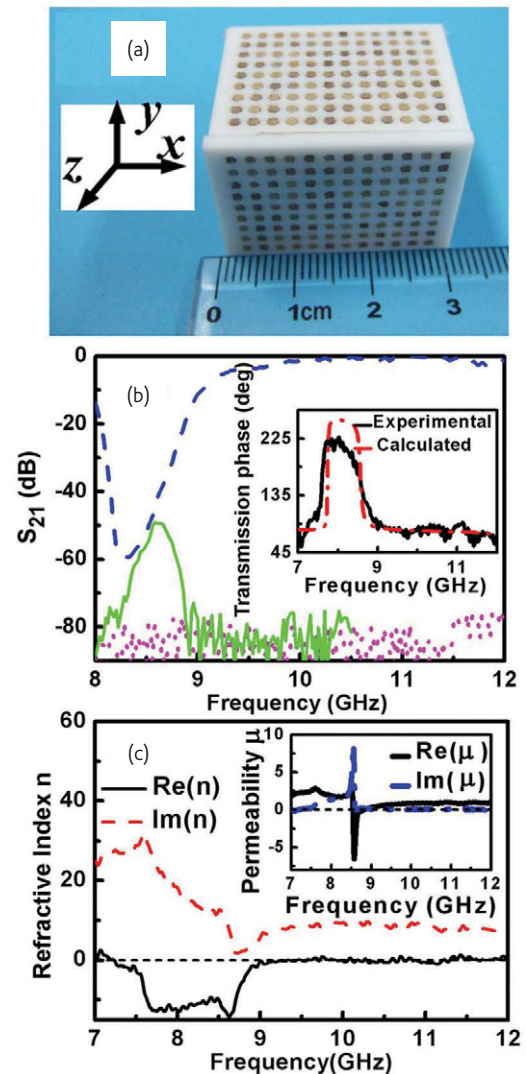


Fig. 3 A three-dimensional dielectric composite with isotropic negative permeability. (a) Photograph of BST cubes arrayed in Teflon substrate. (b) Transmission for the dielectric cube array only (dashed line), wire array only (dotted line), and the combination of BST cubes and wires (solid line). Inset of Fig. 3(b) shows the measured and calculated transmission phase. (c) Retrieved refractive index and permeability (inset). (Reprinted with permission from³⁷. © 2008 American Physical Society.)

experimentally demonstrated in the microwave region³⁷. The dielectric cube side length l was 1.0 mm for a lattice constant of 2.5 mm. And the first TE and TM resonance modes, i.e., magnetic and electric resonances were determined by transmission measurements at 6.12 and 8.28 GHz respectively. Using smaller cubes ($l = 0.75$ mm) with a magnetic resonance near 8.5 GHz, in conjunction with an electric response from metallic wires, researchers fabricated double negative media. The results of transmission measurements are displayed in Fig. 3b and the retrieved electromagnetic parameters (Fig. 3c) further verified the negative permeability near the first Mie resonance.

A rectangular dielectric block⁴³ and piezoelectric disks⁴⁴ were also experimentally verified to design very low-loss magnetic metamaterials.

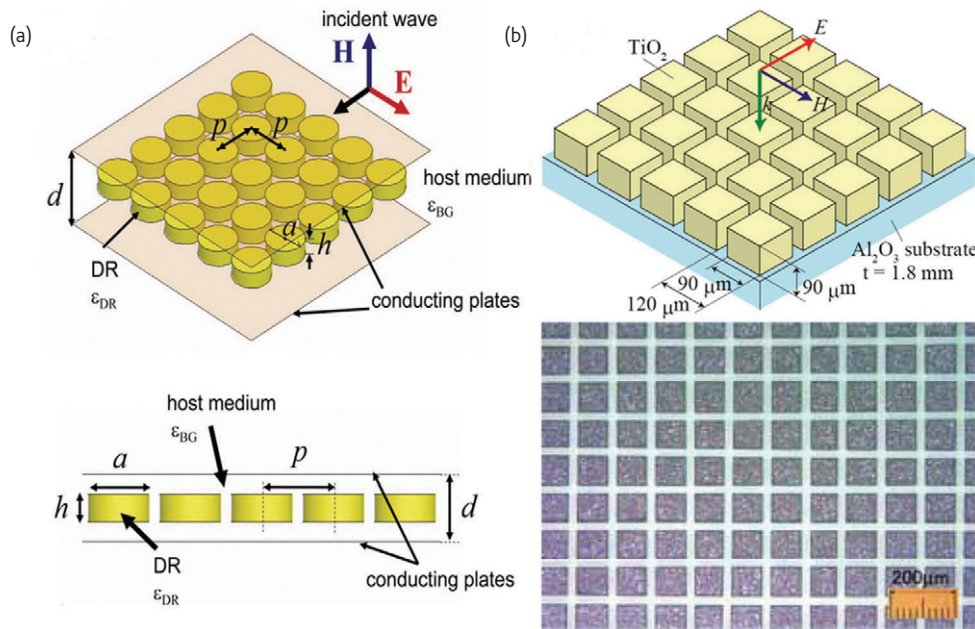


Fig. 4 Schematic of metamaterials based on Mie resonance. (a) A two-dimensional lattice structure for one dielectric-resonator in the cutoff microwave waveguide. (Reprinted with permission from⁴⁵. © 2007 IEEE.) (b) Terahertz metamaterial consisting of polycrystalline TiO_2 cubes-arrays on the Al_2O_3 substrate. (Reprinted with permission from⁴⁸. © 2008 Metamaterials.)

Also a two-dimensional square lattice of dielectric disk inserted between two metallic parallel-plate waveguide (Fig. 4a) was also used to demonstrate negative refraction, where the macroscopic behavior of dielectric disk provides negative effective permeability and the waveguide plays a role in a TE cut-off waveguide leading to negative effective permittivity⁴⁵. A dielectric block [(Zr,Sn) TiO_4 ceramics, dielectric constant 36.7] with a thin metallic rod screwed inside was proposed to fabricate gradient metamaterial lenses and numerically demonstrated to deflect and focus the incident plane waves⁴⁶. Dielectric-resonator-based composite right/left-handed transmission lines used to the design of leaky wave antenna can alleviate the significantly large conducting loss and increase the radiation efficiency⁴⁷. Terahertz metamaterials based on the Mie resonance of polycrystalline TiO_2 cubes-arrays on the Al_2O_3 substrate (Fig. 4b) were also experimentally demonstrated by Shibuya *et al.*⁴⁸, in which the negative permeability and permittivity occur around 0.28 and 0.38 THz, respectively.

A three-dimensional collection of polaritonic spheres was proposed to obtain isotropic negative effective permeability near the first Mie resonance at infrared frequencies⁴⁹. The calculated effective parameters (LiTaO_3 crystal) reported in this reference are shown in Fig. 5 and the isotropy of electromagnetic properties was also verified by a comparison with a full multiple scattering approach. Semiconductor nanoparticles, such as CuCl with a $3P$ exciton line at 386.93 nm, Cu_2O with a $2P$ exciton⁵⁰, and GaP ⁵¹ were also suggested to realize negative permeability within and below the optical region. Metal nanoclusters possessing large permittivity at visible frequency can also be used to obtain magnetic Mie resonance^{52, 53}.

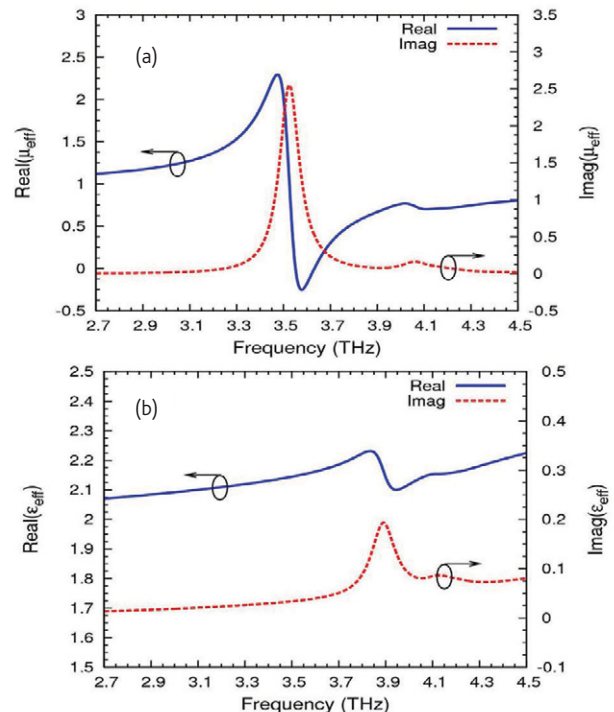


Fig. 5 The calculated effective relative permeability (a) and permittivity (b) of a collection of LiTaO_3 spheres. (Reprinted with permission from⁴⁹. © 2005 American Physical Society.)

Similar to spherical or cubic dielectric elements, the cylindrical particles can also generate the Mie electromagnetic resonances. The most important issue is to determine the resonant modes. For

a TE polarization (E field perpendicular to the rod axis), the lowest Mie resonance mode (TE_0) corresponds to the magnetic response, resulting in negative permeability values. A two-dimensional array of ferroelectric rods^{28, 54} and polaritonic rods⁵⁵ were proposed to obtain negative effective permeability⁵⁶, which can be considered as the TE_0 mode. For TM polarization (E field parallel to the rod axis), the lowest two Mie resonances modes, TM_0 and TM_1 , correspond to the electric and magnetic responses, and consequently lead to negative permittivity and permeability, respectively. The electromagnetic field distribution displayed for the TM_1 mode (Fig. 6) can further clarify the magnetic resonance mechanism⁵⁷. The electric field is distributed along the $\pm z$ directions with opposite signs along the propagation direction (Fig. 6b), accounting for a strong circular displacement current (Fig. 6d). Such displacement current results in a large magnetic field along the y axis (Fig. 6c), which corresponds to the TM_1 mode.

Electric response

An electric response can be accomplished with simpler metallic structures, such as uncoupled rods or strips. The first method to obtain negative permittivity is the bulk metals at optical frequencies, where conduction electrons can be assumed to be reasonably free and plasma-like behavior is responsible for a negative dielectric permittivity at frequencies less than the plasma frequency⁵⁸. Usually, the plasma frequencies of metals are at ultraviolet frequencies and dissipation is small. As the frequency is much lower than the plasma frequency, the imaginary part of the complex permittivity increases dramatically while very large negative values of the real part are obtained.

Pendry *et al.*⁵⁹ suggested a metallic wire array structure to realize a plasma-like state. With such a configuration, the negative permittivity frequency range can be tuned by the lattice constant and the wire diameter in the low frequency spectral region even at microwave frequencies. Additionally, negative dielectric permittivity can also be obtained in more ordinary dielectric media with bound charges, within a frequency band above a resonance frequency, where the resonant Lorentz permittivity occurs⁵⁸.

Another method is to use the electric resonant mode of the Mie resonance of dielectric particles. For the dielectric sphere or cube, it can be equivalent to a dipole at the second resonant mode as exemplified by the field mapping shown in Fig. 1. For a dielectric column particle, it can be equivalent to an electric dipole at the first resonance mode (TM_0) and can result in negative permittivity.

Negative refraction

The mechanisms of electric and magnetic resonances in dielectric particles (spheres, cubes or rods) have been analyzed above. Negative refraction can be fulfilled by combing the two resonances together. However, the first electric resonance (TM mode) is at a higher frequency than the fundamental magnetic resonance (TE mode) for the identical sphere. Due to the different resonance frequencies of TE and TM modes in the different-sized particles, we can consider the conditions when the first lowest resonance of TM_{011} mode related to a bigger sphere coincides with the TE_{011} resonance in a smaller sphere. Recently, Vendik *et al.*^{60, 61} numerically studied an artificial double negative media whose basic unit cell is composed by two

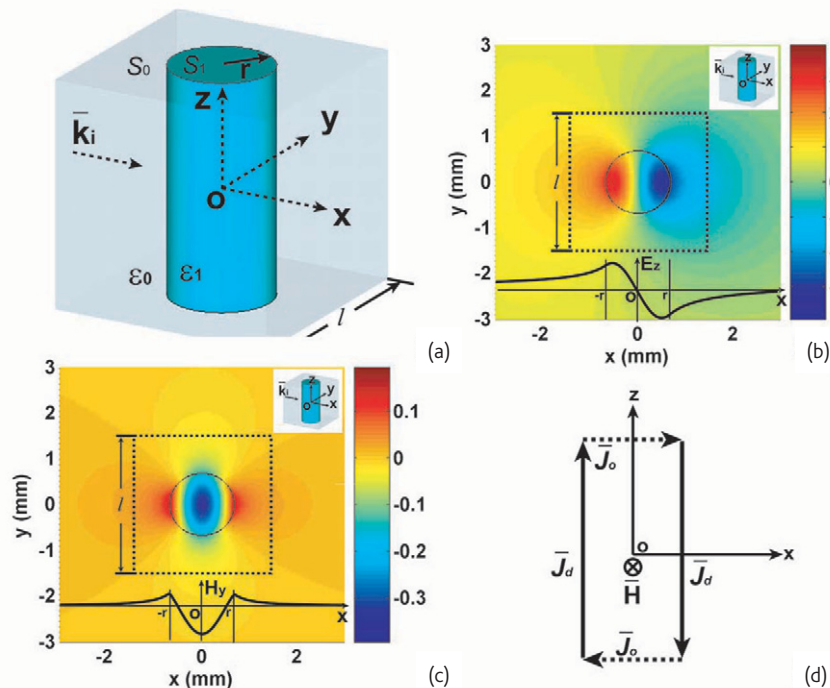


Fig. 6 Electric and magnetic field distributions in a dielectric rod at the second resonant mode (TM_1 mode). (a) Unit cell configuration. (b) Electric field distribution. (c) Magnetic field distribution. (d) Equivalent current ring. (Reprinted with permission from⁵⁷. © 2007 American Physical Society.)

dielectric spheres of different sizes. The larger sphere was used for the negative permeability while the small one allows achieving a negative permittivity in the same microwave frequency band. At the same time, two sets of spheres, having the same size but different materials, were also developed to realize negative refraction⁶². More recently, a three-dimensional isotropic negative-index composite at infrared or visible frequencies was reported^{51, 63-66}. The proposed homogeneous isotropic structures consist of dielectric spheres (gallium phosphide) embedded randomly in a negative permittivity host medium (Cesium)⁵¹, or two interpenetrating lattices of spheres⁶³⁻⁶⁶. One lattice ensures a negative permeability using a polaritonic material (LiTaO₃, SiC, CuCl) and the other lattice creates a negative permittivity effect by using a plasmonic material (n-type Ge, Au, MgB₂). Negative refraction index effect exists not only in the situation of a regular lattice arrangement but also for randomly distributed nanoparticles when the losses are ignored. However, the numerical results also demonstrated that the negative refraction could not be achieved owing to the large imaginary part of the wave vector corresponding to evanescent rather than propagating waves when the losses of the constitutive materials were taken into account.

Another method to fabricate isotropic LHMs based on Mie resonance is using only one kind of micron-scale non-magnetic coated spheres⁶⁷⁻⁶⁹. The underlying physical mechanisms correspond to a negative effective permeability effect due to polaritonic sphere core while a negative effective permittivity effect results from an electric-dipole resonance of sphere coating on its outer surface whose dispersion follows a Drude model. For an isolated sphere, an electric dipole resonance can be driven when its material permittivity is -2 . Since this permittivity value is negative, the electric field is evanescent within the sphere so that such electric dipole resonance is a surface resonance in contrast to the volume effect of the magnetic resonance. Therefore, the coating can be designed to have a negative permittivity. Note that the magnetic resonance of the core is hardly affected, as long as the permittivity of the coating remains small in comparison to the large permittivity of the core. The spheres with a core of a polaritonic crystal LiTaO₃ and the coated thin layer of a Drude model semiconductor (or a polaritonic material) were used to demonstrate isotropic negative refraction⁷⁰. The calculated effective electromagnetic parameters are shown in Fig. 7. Such three-dimensional LHMs consisting of metal-coated semiconductor spheres can be used to realize subwavelength imaging⁷¹ and electromagnetic transparency^{72, 73}.

Besides dielectric spheres array, the electric and magnetic Mie resonances in dielectric rods can also be used to achieve negative permittivity and permeability values. Under TM illumination, a resonant permittivity due to the TM₀ mode excitation and a resonant permeability due to the TM₁ mode excitation can be used to realize negative permittivity and permeability, respectively. Schuller *et al.*⁷⁴ experimentally and numerically observed and identified the Mie

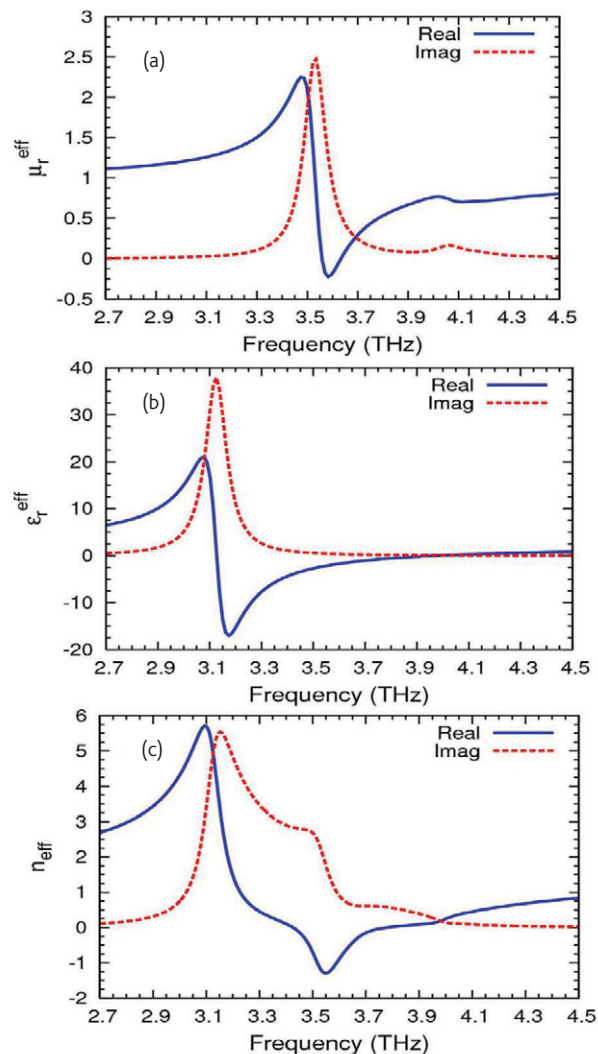


Fig. 7 The effective (a) permeability, (b) permittivity, and (c) index of a collection coated spheres. The cores are made of LiTaO₃ with radius 4 μm , and the coatings are a Drude material with radius 0.7 μm . (Reprinted with permission from⁷⁰. © 2006 American Physical Society.)

resonance modes of SiC particles at mid-IR under various polarization conditions. Also they proposed to obtain a negative refractive index by combining the two resonances of TM₀ and TM₁ modes (Fig. 8).

A theory on the electric and magnetic dipole activities of dielectric rods in s-polarized light was presented recently. The authors claimed that large wavelength-to-period ratios do not necessarily result in an isotropic metamaterial. They also suggested that silicon rod arrays could exhibit a true metamaterial left handed dispersion branch in the visible to mid-IR despite the moderate value of the refractive index ($n \sim 3.5$)⁷⁵. Such a conclusion is interesting by considering Mie resonance in moderate permittivity materials in optics. It has however to be checked by experiments in order to discriminate negative refraction effects resulting from the conventional band folding in the diffraction regime⁷⁶ from pure left handed branch effects in the

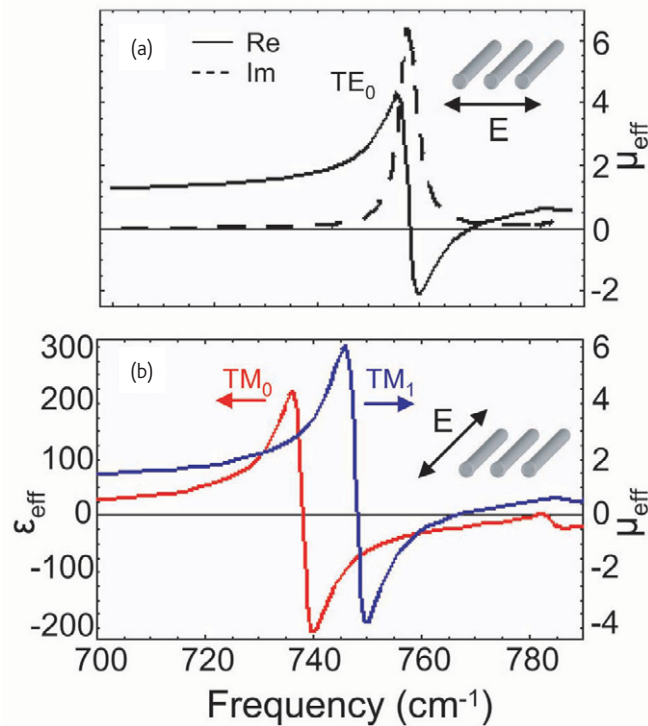


Fig. 8 (a) Calculated effective permeability for a normal incidence TE illuminated array of infinitely long SiC rods. (b) Calculated permittivity (permeability) due to excitation of the zeroth (first) order TM mode. (Reprinted with permission from⁷⁴. © 2007 American Physical Society.)

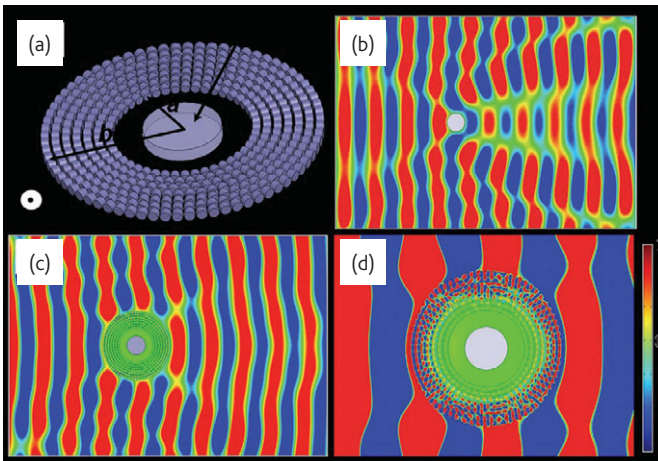


Fig. 9 (a) Schematic of a terahertz all-dielectric cloak. Steady-state E_z pattern calculated at 0.58 THz for a copper rod without (b) and with cloak (c). (d) Magnified view of the field pattern of (c). (Reprinted with permission from⁷⁷. © 2008 Optical Society of America.)

long wavelength regime. A verification of negative refraction in a TM illuminated array of large permittivity ceramic rods was experimentally verified at microwave frequencies, corresponding to the combination of TM_0 and TM_1 modes⁵⁷.

All-dielectric cloaks

Conformal transformation of electromagnetic domains has been proposed as an exciting approach to control the flow of propagating

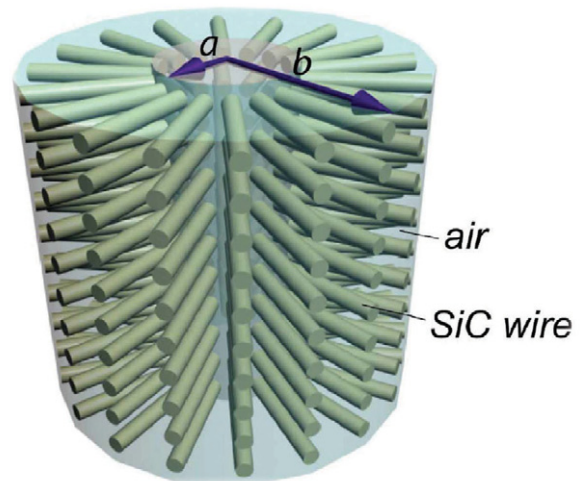


Fig. 10 Schematic of a cylindrical non-magnetic cloak for TE polarization at mid-infrared. (Reprinted with permission from⁷⁸. © 2008 Optical Society of America.)

waves and realize invisibility cloak⁶. Effective permeability can be less than unity around the magnetic resonance and such metamaterials have been suggested to construct invisibility cloak^{7, 8}. An all-dielectric cloak (Fig. 9) consisting of radially positioned micrometer-sized ferroelectric cylinders was suggested to perform cloaking at 0.58 THz, which exhibits a strong magnetic resonance based on Mie theory⁷⁷.

At last, Silicon Carbide (SiC) rod, a polaritonic material with phonon resonance bands centered around 12.5 μm , was also suggested to built transparency cloak (Fig. 10) at mid-infrared with the TE resonance mode⁷⁸. To sum up, an all-dielectric configuration provides an attractive route for designing cloaking devices at microwave, terahertz and infrared frequencies.

Tunable Mie resonance-based metamaterials

As seen in the previous sections, resonance effects in the electric and magnetic responses appear as a necessary condition for fabricating left-handed metamaterials. Such resonances are strongly dependent on the geometrical dimensions and on the dielectric properties of the constitutive elements. Usually negative values can only be achieved over a narrow frequency range near the resonances, especially for the magnetic resonance. From the application point of view, and for a deeper understanding of the intrinsic properties of negative media, it is desirable to implement structures with tunable and reconfigurable resonant properties⁷⁹. Some tunable metamaterials based on the metallic structures have been proposed by modifying the locally dielectric or permeability environment. For example, a control of the electric and magnetic responses of SRRs and related configurations was experimentally demonstrated through photoexcitation of free carriers in a GaAs substrate⁸⁰, electrically or magnetically controlled liquid crystals^{81, 82}, along with electroreological fluids^{83, 84}, ferroelectric⁸⁵, ferromagnetic materials⁸⁶⁻⁸⁹ and other methods⁹⁰. All these examples correspond however to anisotropic tunable metamaterials whereas

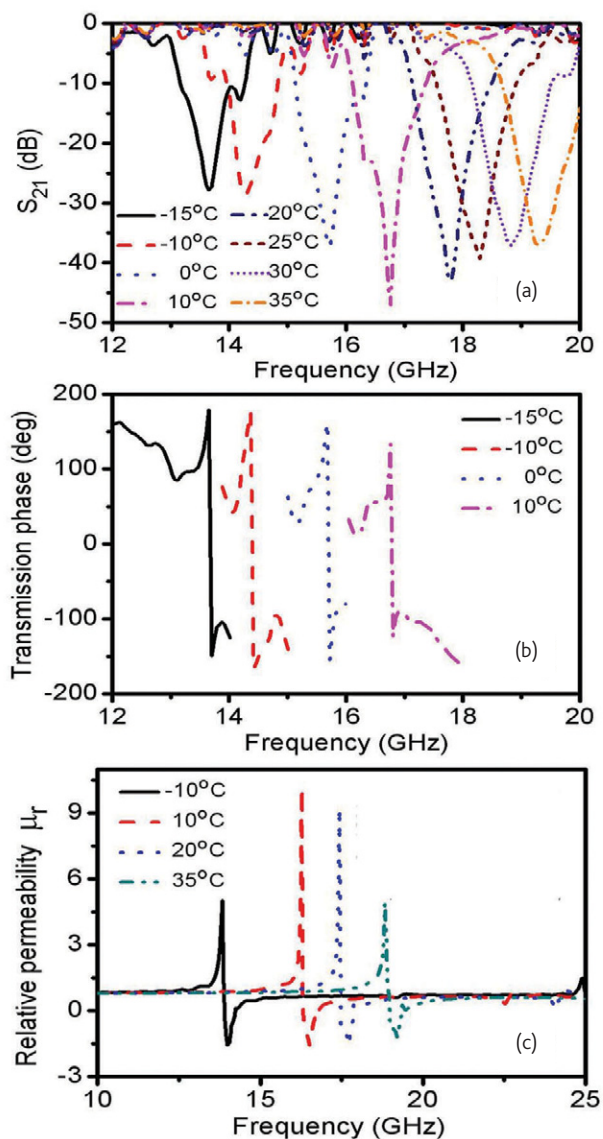


Fig. 11 The actively modulated isotropic negative permeability dielectric composite. (a) Dependence of the first magnetic resonance on the temperature. (b) Dependence of transmission phases on the temperature. (c) Calculated effective permeability under different temperature. (Reprinted with permission from⁹¹. © 2008 American Institute of Physics.)

isotropic properties can be more suitable for potential applications notably for all angle negative refraction.

The first dynamic tuning of isotropic metamaterial relying on Mie resonance has been demonstrated recently by altering the dielectric property of the basic cell⁹¹. As expected from the Mie resonance theory, at the first resonance the dielectric sphere is equivalent to a magnetic dipole with a resonance frequency $\omega \approx \pi c / (r_0 \sqrt{\epsilon_2})$ within the long-wavelength limit. Usually, the permittivity of the high κ ceramic inclusions varies as a function not only of the local field, but also of temperature⁹². Therefore, a variation of the effective permeability of the composite material can be realized by changing

the sample temperature. For a proof of this principle, a simple cubic lattice of ceramic cubes of 0.45 mm side length (BST doped with 5wt% MgO) were arrayed in a Teflon substrate with a lattice constant of 1.25 mm. The microwave scattering parameters were measured under various temperature conditions (Fig. 11a, b). The magnetic resonance corresponding to the first Mie resonance in the dielectric cubes can be continuously and reversibly adjusted from 13.65 GHz to 19.28 GHz with a temperature changing from -15°C to 35°C. The frequency dependence of the effective permeability, displayed in Fig. 11c, shows that negative permeability values can be achieved in a frequency band of about 6 GHz by a temperature variation of 50°C. It is believed that this temperature controlled metamaterial could be used for the design of adaptive three-dimensional metamaterials and invisibility cloaks which exhibit basically a very narrow fractional bandwidth of the order of 1%⁹³.

Another method used to adjust the negative refraction of Mie resonance is to alter the dielectric property of the background medium. Khoo *et al.*⁹⁴ proposed nanospheres dispersed liquid crystals to realize tunable negative-zero-positive index of refraction in the optical and terahertz regimes.

Outlook

As an alternative method for the design of electromagnetic metamaterials, the dielectric particles show several advantages, notably in terms of isotropic parameters, and the fabrication techniques targeting at higher frequencies of operation. Although several experimental demonstrations have allowed the verification of the first principles at microwave and terahertz frequencies, it appears that the research on this area is at a very primary stage with numerous theoretical and numerical studies. Further experimental works are expected at mid-term in order to demonstrate the possibility of fabricating isotropic negative index material notably in the infrared and visible frequency ranges. Towards this goal the challenging issues are the preservation of large dielectric constant and low loss in these frequency ranges, which appear as the necessary condition to operate in the long wavelength regime. The introduction of active materials may alleviate or even overcome the problem of intrinsic losses⁹⁵. At last the inexpensive chemical methods, such as colloidal crystallization, may be suitable for the synthesis of nanoparticles^{96, 97}. Although much work is needed before practical implementations are possible, dielectric metamaterials are a promising candidate for real-world application of the many exciting opportunities provided by electromagnetic metamaterials. mt

Acknowledgments

This work is supported by the National Science Foundation of China under Grant Nos. 50425204, 50621201, 50632030, 60608016 and 10774087, and by the State Key Lab of Tribology under Grant No. SKLT 08B12. D.L. would like also to thank the Delegation Générale pour l'Armement for its support in the framework of the contract 06.34.021.

Reference

1. Pendry, J. B., *Nature Mater.* (2006) **5**, 763.
2. Shelby, R. A., *et al.*, *Science* (2001) **292**, 77.
3. Houck, A. A., *et al.*, *Phys. Rev. Lett.* (2003) **90**, 137401.
4. Pendry, J. B., *Phys. Rev. Lett.* (2000) **85**, 3966.
5. Fang, N., *et al.*, *Science* (2005) **308**, 534.
6. Pendry, J. B., *et al.*, *Science* (2006) **312**, 1780.
7. Schurig, D., *et al.*, *Science* (2006) **314**, 977.
8. Cai, W., *et al.*, *Nat. Photonics* (2007) **1**, 224.
9. Wiltshire, M. C. K., *et al.*, *Science* (2001) **291**, 849.
10. Zhang, F. L., *et al.*, *Appl. Phys. Lett.* (2008) **93**, 083104.
11. Dolling, G., *et al.*, *Science* (2006) **312**, 892.
12. Linden, S., *et al.*, *Science* (2004) **306**, 1351.
13. Liu, H., *et al.*, *Adv. Mater.* (2008) **20**, 2050.
14. Dolling, G., *et al.*, *Opt. Lett.* (2007) **32**, 53.
15. Pendry, J. B., *et al.*, *IEEE Trans. Microw. Theory Tech.* (1999) **47**, 2075.
16. Smith, D. R., *et al.*, *Phys. Rev. Lett.* (2000) **84**, 4184.
17. Huangfu, J., *et al.*, *Appl. Phys. Lett.* (2004) **84**, 1537.
18. Zhang, F. L., *et al.*, *IEEE Trans. Microw. Theory Tech.* (2008) **56**, 2566.
19. Enkrich, C., *et al.*, *Phys. Rev. Lett.* (2005) **95**, 203901.
20. Zhang, S., *et al.*, *Phys. Rev. Lett.* (2005) **94**, 037402.
21. Shalaev, V. M., *et al.*, *Opt. Lett.* (2005) **30**, 3356.
22. Zhou, X., and Zhao, X. P., *Appl. Phys. Lett.* (2007) **91**, 181908.
23. Dolling, G., *et al.*, *Opt. Lett.* (2006) **31**, 1800.
24. Baena, J. D., *et al.*, *Appl. Phys. Lett.* (2006) **88**, 134108.
25. Gay-Balmaz, P., and Martin, O. J. F., *Appl. Phys. Lett.* (2002) **81**, 939.
26. Koschny, T., *et al.*, *Phys. Rev. B* (2005) **71**, 21103.
27. Veselago, V. G., and Narimanov, E. E., *Nat. Mater.* (2006) **5**, 759.
28. O'Brien, S., and Pendry, J. B., *J. Phys.: Condens. Matter* (2002) **14**, 4035.
29. Holloway, C. L., *et al.*, *IEEE Trans. Antennas Propag.* (2003) **51**, 2596.
30. Shalaev, V. M., *Nat. Photon.* (2007) **1**, 41.
31. Padilla, W. J., *et al.*, *Materials Today* (2006) **9**, 28.
32. Soukoulis, C. M., *et al.*, *Adv. Mater.* (2006) **18**, 1941.
33. Engheta, N., and Ziolkowski, R. W., (eds.), *Electromagnetic Metamaterials: Physics and Engineering Explorations*, Wiley-IEEE Press, New Jersey, USA, (2006).
34. Marques, R., Martin, F., and Sorolla, M., *Metamaterials with Negative Parameters: Theory, Design, and Microwave Applications*, Wiley-Interscience Press, New Jersey, USA, (2007).
35. Jackson, J. D., *Classical Electrodynamics*, 2nd ed., Wiley, New York, USA, (1999).
36. Bohren, C. F., and Huffman, D. R., *Absorption and Scattering of Light by Small Particles*, Wiley-Interscience, New York, USA, (1983).
37. Zhao, Q., *et al.*, *Phys. Rev. Lett.* (2008) **101**, 027402.
38. Lewin, L., *Proc. Inst. Electr. Eng.* (1947) **94**, 65.
39. Jylha, L., *et al.*, *J. Appl. Phys.* (2006) **99**, 043102.
40. Contopanagos, H. F., *et al.*, *J. Opt. Soc. Am. A* (1999) **16**, 1682.
41. Houzet, G., *et al.*, *Appl. Phys. Lett.* (2008) **93**, 053507.
42. Kittel, C., *Introduction to Solid State Physics*, 7th ed., John Wiley and Sons Inc., New York, USA, (1996).
43. Popa, B.I., and Cummer, S.A., *Phys. Rev. Lett.* (2008) **100**, 207401.
44. Acher, O., *et al.*, *Appl. Phys. Lett.* (2008) **93**, 032501.
45. Ueda, T., *et al.*, *IEEE Trans. Microw. Theory Tech.* (2007) **55**, 1280.
46. Lin, X. Q., *et al.*, *Appl. Phys. Lett.* (2008) **92**, 131904.
47. Ueda, T., *et al.*, *IEEE Trans. Microw. Theory Tech.* (2008) **56**, 2259.
48. Shibuya, K., *et al.*, *Terahertz metamaterials composed of TiO₂ cube arrays*, Presented at 2nd International Congress on Advanced Electromagnetic Materials in Microwaves and Optics, Pamplona, Spain, September 21-26, 2008.
49. Wheeler, M. S., *et al.*, *Phys. Rev. B* (2005) **72**, 193103.
50. Yannopapas, V., and Vitanov, N. V., *Phys. Rev. B* (2006) **74**, 193304.
51. Seo, B. J., *et al.*, *Appl. Phys. Lett.* (2006) **88**, 161122.
52. Wu, Q., and Park, W., *Appl. Phys. Lett.* (2008) **92**, 153114.
53. Rockstuhl, C., *et al.*, *Phys. Rev. Lett.* (2007) **99**, 017401.
54. Felbacq, D., and Bouchitte, G., *New J. Phys.* (2005) **7**, 159.
55. Huang, K. C., *et al.*, *Appl. Phys. Lett.* (2004) **85**, 543.
56. Felbacq, D., and Bouchitte, G., *Phys. Rev. Lett.* (2005) **94**, 183902.
57. Peng, L., *et al.*, *Phys. Rev. Lett.* (2007) **98**, 157403.
58. Ramakrishna, S. A., *Rep. Prog. Phys.* (2005) **68**, 449.
59. Pendry, J. B., *Phys. Rev. Lett.* (1996) **76**, 4773.
60. Vendik, O. G., and Gashinova, M. S., in Proceedings of the 34th European Microwave Conference, Amsterdam (IEEE Press, Piscataway, NJ, 2004), Vol. 3, pp. 1209-1212.
61. Vendik, I. B., *et al.*, *Tech. Phys. Lett.* (2006) **32**, 429.
62. Ahmadi, A., and Mosallaei, H., *Phys. Rev. B* (2008) **77**, 045104.
63. Yannopapas, V., *Phys. Rev. B* (2007) **75**, 035112.
64. Kussow, A. G., *et al.*, *Phys. Stat. Sol. B* (2008) **245**, 992.
65. Kussow, A. G., *et al.*, *Phys. Rev. B* (2007) **76**, 195123.
66. Yannopapas, V., *Appl. Phys. A* (2007) **87**, 259.
67. Qiu, C. W., and Gao, L., *J. Opt. Soc. Am. B* (2008) **25**, 1728.
68. Yannopapas, V., *Phys. Stat. Sol. (RRL)* (2007) **1**, 208.
69. Alu, A., and Engheta, N., *J. Appl. Phys.* (2005) **97**, 094310.
70. Wheeler, M. S., *et al.*, *Phys. Rev. B* (2006) **73**, 045105.
71. Yannopapas, V., *J. Phys.: Condens. Matter* (2008) **20**, 255201.
72. Gao, L., *et al.*, *Phys. Rev. E* (2008) **78**, 046609.
73. Alu, A., and Engheta, N., *Phys. Rev. E* (2005) **72**, 016623.
74. Schuller, J. A., *et al.*, *Phys. Rev. Lett.* (2007) **99**, 107401.
75. Vynck, K., *et al.*, "All-dielectric rod-type metamaterials operating at optical frequencies," <http://arxiv.org/abs/0805.0251> (2008).
76. Fabre, N., *et al.*, *Phys. Rev. Lett.* (2008) **101**, 073901.
77. Gaillot, D. P., *et al.*, *Opt. Express* (2008) **16**, 3986.
78. Cai, W., *et al.*, *Opt. Express* (2008) **16**, 5444.
79. Chen, H. T., *et al.*, *Nature* (2006) **444**, 597.
80. Padilla, W. J., *et al.*, *Phys. Rev. Lett.* (2006) **96**, 107401.
81. Zhao, Q., *et al.*, *Appl. Phys. Lett.* (2007) **90**, 011112.
82. Zhang, F. L., *et al.*, *Appl. Phys. Lett.* (2008) **92**, 193104.
83. Hou, B., *et al.*, *Opt. Express* (2005) **13**, 9149.
84. Huang, Y., *et al.*, *Prog. Nat. Sci.* (2008) **18**, 907.
85. Hand, T. H., and Cummer, S. A., *J. Appl. Phys.* (2008) **103**, 066105.
86. Kang, L., *et al.*, *Appl. Phys. Lett.* (2008) **93**, 171909.
87. Kang, L., *et al.*, *Opt. Express* (2008) **16**, 8825.
88. Kang, L., *et al.*, *Opt. Express* (2008) **16**, 17269.
89. Zhao, H. J., *et al.*, *Appl. Phys. Lett.* (2007) **91**, 131107.
90. Chen H., *et al.*, *Appl. Phys. Lett.* (2006) **89**, 053509.
91. Zhao, Q., *et al.*, *Appl. Phys. Lett.* (2008) **92**, 051106.
92. Vendik, O. G., and Zubko, S. P., *J. Appl. Phys.* (1997) **82**, 4475.
93. Gaillot, D. P., *et al.*, *New J. Phys.* (2008) **10**, 115039.
94. Khoo, I. C., *et al.*, *Opt. Lett.* (2006) **31**, 2592.
95. Gordon, J. A., and Ziolkowski, R. W., *Opt. Express* (2007) **15**, 2622.
96. Huang, X. G., *et al.*, *Langmuir* (2007) **23**, 8695.
97. Li, W., *et al.*, *Langmuir* (2008) **24**, 13772.